GEOPHYSICAL RESEARCH LETTERS, VOL. 22, NO. 8, PAGES 937-940, APRIL 15, 1995

Decadal-to-centennial-scale climate variability: Insights into the rise and fall of the Great Salt Lake

Michael E. Mann

Department of Geology and Geophysics, Yale University, New Haven, Connecticut

Upmanu Lall

Utah Water Research Laboratory, Utah State University, Logan, Utah

Barry Saltzman

Department of Geology and Geophysics, Yale University, New Haven, Connecticut

Abstract. We demonstrate connections between decadal and secular global climatic variations, and historical variations in the volume of the Great Salt Lake. The decadal variations correspond to a low-frequency shifting of storm tracks which influence winter precipitation and explain nearly 18% of the interannual and longer-term variance in the record of monthly volume change. The secular trend accounts for a more modest ~1.5% of the variance.

Introduction

Prospects of anthropogenic climate change have renewed interest in the study of low frequency variability in hydro-climatic processes [*Aguado et al.*, 1992; *Rasmusson and Arkin*, 1993; *Lins and Michaels*, 1994]. Permanent closed basin lakes are unique in that they reflect a precarious long term balance of precipitation and evaporation in an arid region. Several studies have established linkages between regional hydrological patterns and large-scale atmospheric circulation [*Rasmusson and Arkin*, 1993; *Lins*, 1985; *Cayan and Peterson*, 1989; *Ely et al.*, 1994]. Here, we demonstrate the connection between climatic signals and the fluctuations in the volume of the closed-basin Great Salt Lake (GSL). The GSL (Figure 1a) provides a useful case study because of its dramatic historical fluctuations (Figure 1b). The monthly volume change (ΔV–Figure 1c) is a measure of the response to hydrological fluxes. We use monthly streamflow and precipitation records to measure the hydrological forcing of the GSL, and employ a spatiotemporal analysis of gridded, century-long records of monthly surface temperature (T_s) and sea level pressure (P_s) to isolate quasiperiodic climatic signals. Variations in P_s reflect changes in atmospheric circulation that affect ΔV largely through precipitation. Evaporation is associated with T_s, as well as moisture transport, cloud cover, and wind patterns tied to the P_s field. Our spatiotemporal analysis of hydro-climatic data contrasts with conventional distributed approaches to modeling hydrological systems.

Paper number 95GL00704
0094-8534/95/95GL-00704$03.00

Data and Methods

The Silver-Lake Brighton (SLB) station provides a long record of precipitation in the GSL basin immune from local lake and rain shadow effects. The Blacksmith Fork at Hyrum (BFH) river gauge provides the longest record of streamflow which enters into the GSL, free of regulation or diversion. SLB and BFH are located near the south and north ends, respectively, of the GSL basin (see Figure 1a). The at-site records (ΔV, SLB precipitation, and BFH streamflow) indicate broad power on interannual, interdecadal, and secular time scales [*Lall and Mann*, 1993]. To identify large scale climatic signals that may lead to regional hydrological variability, we perform spatiotemporal analyses of the P_s and T_s fields. We used gridded P_s (from 1899-1990, on a 5^o by 5^o grid) over the continental U.S. and surrounding region [see *Jenne*, 1975]. and global gridded T_s (land air and sea-surface temperature anomaly from 1890-1990, 5^o by 5^o grid) [see *Jones and Briffa*, 1992]. The T_s analysis is taken from *Mann and Park* [1994] who describe the analysis technique (summarized below) that is applied here independently to the P_s dataset.

The analysis is performed on standardized time series ${x_n}^{(m)}$ ($n = 1, \ldots N$ indexes time, m indexes the grid-point) for which the long-term mean is removed and the time series is divided by its long-term standard deviation. Standardized time series are transformed by multitaper spectral analysis [*Thomson*, 1982], calculating K independent spectral estimates of each time series at each frequency f. The K eigenspectral estimates are confined within the frequency band $f \pm p/N\Delta t$ where $p = 2K - 1$. We use $K = 3$ (bandwidth $2/N\Delta t$, Δt=1 month). A complex singular-value decomposition (SVD) of the the $M \times K$ matrix of spectral estimates, $\mathbf{A}(f) = \left[{Y_k}^{(m)}\right]$ is performed at each frequency f in the range $0 < f < 0.5$ cycles/year, each row calculated from a different grid-point time series, each column using a different taper. At each frequency, the SVD returns K orthogonal modes. Potential signals are indicated by a

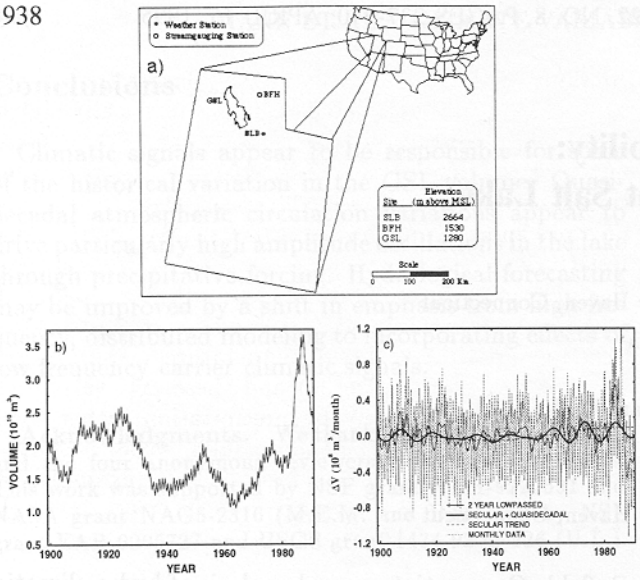

Figure 1. (a) Site Map showing Great Salt Lake (GSL), Silver-Lake Brighton (SLB) station monthly precipitation, and the Blacksmith Fork at Hyrum (BFH) river gauge of monthly streamflow. (b) Great Salt Lake volume record from 1899-1990 (in units of m^3). The most notable feature observed is the large fluctuation of the 1980s. (c) ΔV monthly time series (dotted–units of m^3/month) from 1899-1990. The annual cycle is the most prominent feature in the record, but note the interannual and longer time scale variability revealed by the 2-year lowpassed curve (thin solid) and the specific contributions indicated by the trend (dashed curve) and trend combined with the quasidecadal (thick curve) signal reconstruction (see "Data and Methods"). The 1980's peak may largely be associated with constructive interference of the secular trend, quasidecadal and interannual oscillations.

narrow frequency band ($f \pm p/N\Delta t$) within which the principal mode explains a large fraction of the variance in the band. Statistical signficance is determined from Monte Carlo simulations.

The left eigenvectors of the principal mode determines the slowly-varying complex time envelope $E(t)$, describing a quasiperiodic oscillation of the form, $y(t) = \Re\{E(t)\exp(ift)\}$ at frequency f. $E(t)$ is described by $K = 3$ complex spectral degrees of freedom. The right eigenvector determines relative amplitude and phase of the oscillation spatially. A chosen phase of the cycle describes a particular pattern of positive and negative anomalies.

Signals in *both* P_s and T_s are observed on 2.2 year quasibiennial, 4-5 year interannual, 10-11 year quasidecadal and secular time scales (Figure 2). These signals are found to be seasonally-robust based on independent warm and cold season analyses, but are most influential during the cold season when synoptic variance is greatest. Statistical significance is insensitive to dropping the first/last 10 years of data from the analysis. We have less confidence in peaks that are significant for only one of the climatic fields. These include the 16-20 year peak in global T_s [see *Mann and Park*, 1993;1994] associated with *interdecadal* variability that may have a source region in the Pacific [e.g., *Trenberth*, 1990; *Graham*, 1994; *Latif and Barnett*, 1994] but for which we can not as yet determine a consistent influence on continental U.S. climate. We focus on quasidecadal and secular signals; interannual variability in the GSL and its relation to the El Nino/Southern Oscillation is discussed elsewhere by *Lall and Moon* [1994].

We independently reconstruct [see *Park and Maasch*, 1993] the quasiperiodic oscillation present in the at-site records at the significant quasidecadal and secular frequencies. Each time-reconstruction (P_s, T_s, and the three at-site records) is statistically independent, and mutual correlation is determined from the spectral coherence [e.g., *Mann and Park*, 1993].

GSL and climatic signals

Quasidecadal (10-11 year period) signals have been observed in gridded global surface temperature [*Mann and Park*, 1994], North Atlantic sea level pressure, winds, and marine and air temperature [*Deser and Blackmon*, 1993] U.S. temperature [*Dettinger and Ghil*, 1991], U.S. streamflow [*Guetter and Georgakakos*, 1993], and equatorial Atlantic sea surface temperatures [*Houghton and Tourre*, 1992] as well as Great Basin precipitation [*Eischeid et al.*, 1985]. While a connection has been suggested between the ~11 year sunspot cycle and decadal variability in atmospheric circulation [*Labitzke and van Loon*, 1988], U.S. precipitation [*Currie and O'Brien*, 1992], and GSL volume [*Willet and Prohaska*, 1987], our analysis argues against such an explanation for the variability described here (Figure 3a). Empirical [e.g., *Deser and Blackmon*, 1993; *Mehta and Delworth*, 1994] and theoretical [*Mehta and Delworth*, 1994; *Weaver et al.*, 1991] evidence suggests that such climate variability may have its origins in North Atlantic ocean-atmosphere interaction The quasidecadal global T_s pattern of *Mann and Park* [1994] displays greatest amplitude there with teleconnections that may perturb storm tracks throughout the Northern hemisphere. This signal is coherent with quasidecadal P_s variations over the continental U.S. (both shown in Figure 3b) at $> 95\%$ confidence level.

Variations in ΔV, local precipitation, and streamflow on this time scale are significantly correlated, and are anticorrelated with the local projection of the quasidecadal P_s mode (Figure 3c,d). ΔV lags precipitation slightly, consistent with the expectation of a lagged response between precipitation and snowmelt runoff. The spatial pattern (Figure 3e) [derived from the spatiotem-

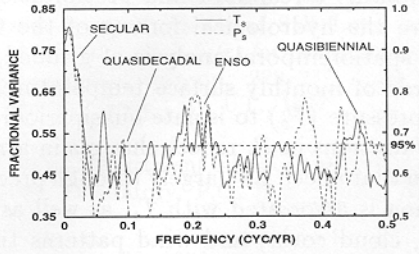

Figure 2. Spectrum of fractional variance explained by the principal mode of the SVD on time scales $\tau > 2$ year for both the P_s data set (dashed) and global T_s data set (solid). The scales (right–P_s, left–T_s) are aligned at the 95% confidence level as calculated from Monte Carlo simulations.

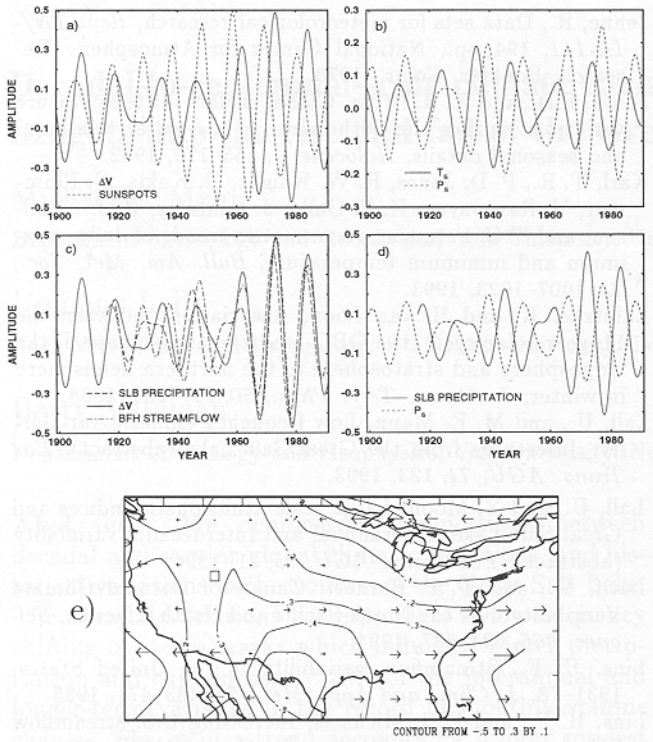

Figure 3. Quasidecadal signal. (a) Variations in ΔV (solid, in units of $2.5 \cdot 10^8$ m^3/month) and sunspot numbers (dashed-vertical scale normalized). The spectral coherence between the two records in this frequency band ($C^2 = 0.03$) is statistically insignificant. (b) Time-domain signals in P_s (dashed) and global temperature (solid) projected onto GSL region. The P_s signal is shown in units of millibars (mb). The temperature oscillation, shown in units of 0.01°C, nearly vanishes locally in the GSL region (see spatial pattern below). (c) Variations in ΔV (solid–units of $2.5 \cdot 10^8$ m^3/month), SLB-precipitation (dashed–units of 2.5 mm/month), and BFH streamflow (dot-dashed–units of 1.5 m^3/s). (d) Variations in SLB precipitation (solid, same units as above) and local projection of P_s mode (dashed–units of mb). The above signals are each correlated at $> 95\%$ confidence levels. Phase discontinuities (during 1930s and near 1960) occur when the complex envelope of the oscillation vanishes, and at-site reconstructions may be contamined by background noise at these times. (e) Large-scale pattern when SLB precipitation is maximum. Position of GSL is indicated (small rectangle with approximate dimensions of the lake). P_s is contoured in units of millibars (mb) with a peak amplitude of about 0.6 mb (peak-to-peak amplitude of 1.2 mb). The global T_s pattern is shown over the same domain. Rightward (leftward) arrows indicate warm (cold) anomalies. Size of arrows scales relative amplitude. Pattern has maximum peak-to-peak amplitude ~ 0.6°C.

poral analysis of P_s] coincident with these conditions indicates a low pressure anomaly from the Great Basin through the Gulf of Mexico. This pattern is associated with an increased likelihood for the winter storm track to shift southward from its typical location to the north (e.g., Montana/Idaho) into the GSL region [*Benson and Thompson*, 1987], leading to enhanced precipitation. The precipitation response appears to be non-linearly related to the P_s variations. For example, the P_s fluctuations of the 1970's, only slightly larger than those of the 1940's, are associated with a dramatically higher response in precipitation, streamflow, and ΔV (Figure 3c). The opposite phase, when ΔV and local precipitation/streamflow are minimum, is associated with high pressure and a diversion of storms from the Great Basin. Relatively moist, cloudy (dry, clear) conditions during the high (low) precipitation phase might serve to inhibit (enhance) evaporation slightly, thus positively reinforcing the signal. Associated temperature variations are locally weak (see Figure 3e) and these ΔV variations are likely driven largely by precipitation rather than evaporation changes [*Lall and Mann*, 1993]. Consistency between T_s and P_s is indicated, for example, by anomalous southerly (northerly) flow about the large cyclonic pressure anomaly associated with warm (cold) anomalies.

On secular time scales, increasing SLB-precipitation is highly correlated with the local decreasing P_s (Figure 4a). The secular temperature mode exhibits the greatest warming before 1940, leading these trends somewhat. Such warming could be expected to lead to enhanced evaporation. Other work [e.g., *Karl et al.*, 1993] suggests that recent warming in this region is marked mostly by higher minimum rather than maximum daytime temperatures which might argue against a strong effect on evaporation. These results, based on linear trends over a shorter time interval (1951-1980), may not, however, extrapolate to the secular variations examined here. Inconsistencies between temperature, precipitation, and streamflow trends over the U.S. [see *Lins and Michaels*, 1994] and influences of long-term changes in cloud cover on evaporation need to be better understood. Consistent, nonetheless, with increased evaporation in the region that accompanies the abrupt secular warming, ΔV tends to decrease until about 1940. Thereafter, increasing precipitation seems to counteract the decline and ΔV increases. The local P_s decrease is associated with a trough that develops over much of the U.S., particularly in the west (Figure 4b), implying increased frequency of mid-latitude storms.

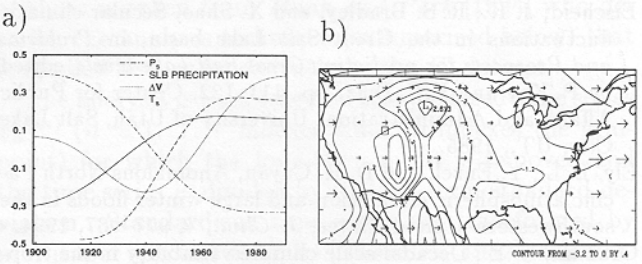

Figure 4. Secular signal. (a) Trends of ΔV (dotted–units of $2.5 \cdot 10^8$ m^3/month), SLB-precipitation (dashed–units of 2.5mm/month), and secular P_s (dot-dashed–units of mb) and T_s (solid–units of °C) modes projected onto GSL region. (b) Large-scale pattern of secular modes. Pattern peak amplitude is -3.3 mb in central Mexico, and nearly as large (-2.6 mb) just northeast of the GSL. Temperature trends are indicated by same convention as above, showing a spatially-varying warming. Maximum amplitude warming in the pattern is 0.85°C off the mid-Atlantic coast, with $\sim 0.4 - 0.5$°C warming over the great basin.

Conclusions

Climatic signals appear to be responsible for some of the historical variation in the GSL volume. Quasi-decadal atmospheric circulation variations appear to drive particularly high amplitude oscillations in the lake through precipitative forcing. Hydrological forecasting may be improved by a shift in emphasis from high frequency, distributed modeling to incorporating effects of low frequency carrier climatic signals.

Acknowledgments. We thank M.D Dettinger, J.Park, and the four anonymous reviewers for helpful comments. This work was supported by NSF grant ATM-9222591 and NASA grant NAG5-2316 (M.E.M. and B.S.) and by NSF grant EAR-9205727 and USGS grant 1434-92-G-226 (U.L.).

References

Aguado, E., D. Cayan, L. Riddle, and M. Roos, Climatic fluctuations and the timing of west coast streamflow, *J. Clim., 5*, 1468–1483, 1992.

Benson, L., and R. S. Thompson, The physical record of lakes in the Great Basin, in *The geology of North America*, edited by W.F. Ruddiman and H.E. Wright Jr., pp. 241–260, Geological Society of America, Boulder, Color., 1987.

Cayan, D. R., and D. H. Peterson, The influence of North Pacific atmospheric circulation on streamflow in the west, in *Aspects of Climate Variability in the Pacific and the Western Americas*, edited by D.H. Peterson, pp. 375–397, American Geophysical Union, Washington, D.C., 1989.

Currie, R. G., and D. P. O'Brien, Deterministic signals in USA precipitation records; II, *Int. J. Climatol., 12*, 281–304, 1992.

Deser, C., and M. Blackmon, Surface climate variations over the North Atlantic ocean during winter: 1900-1989, *J. Clim., 6*, 1743–1753, 1993.

Dettinger, M. D., and M. Ghil, Interannual and interdecadal variability of surface-air temperatures in the United States, *Proceedings of the XVIth Annual Climate Diagnostics Workshop*, pp. 209–214, U.S. Department of Commerce, Los Angeles, Calif., 1991.

Eischeid, J. K., R. S. Bradley, and X. Shao, Secular climatic fluctuations in the Great Salt Lake basin, in *Problems and Prospects for predicting Great Salt Lake levels*, edited by P. Kay and H.F. Diaz, pp. 111–122, Center for Public Affairs and Administration, University of Utah, Salt Lake City, UT., 1985.

Ely, L. L., Y. Enzel, and D. R. Cayan, Anomalous North Pacific atmospheric circulation and large winter floods in the southwestern United States, *J. Clim., 7*, 977–987, 1994.

Graham, N. E., Decadal-scale climate variability in the tropical and North Pacific during the 1970s and 1980s: observations and model results, *Clim. Dyn., 10*, 135–162, 1994.

Guetter, A. K., and K. P. Georgakakos, River outlow of the conterminous United States, 1939-1988, *Bull. Am. Meteorol. Soc., 74*, 1873–1891, 1993.

Houghton, R., and Y. Tourre, Characteristics of low frequency sea-surface temperature fluctuations in the tropical Atlantic, *J. Clim., 5*, 765–771, 1992.

Jenne, R., Data sets for meteorological research, *Rep. TN/-IA-111*, 194 pp., National Center for Atmospheric Research, Boulder, Color., 1975.

Jones, P.D., and K. R. Briffa, Global surface air temperature variations during the 20th century, 1, Spatial, temporal and seasonal details, *Holocene, 1*, 165–179, 1992.

Karl, T. R., P. D. Jones, R. W. Knight, G. Kukla, N. Plummer, V. Razuvayev, K. P. Gallo, J. Lindseay, R. J. Charlson, and T.C. Peterson, Asymmetric trends of daily maximum and minimum temperature, *Bull. Am. Met. Soc., 74*, 1007–1023, 1993.

Labitzke, K. and H. van Loon, Associations between the 11–year solar cycle, the QBO, and the atmosphere, I, the troposphere and stratosphere in the northern hemisphere in winter, *J. Atmos. Terr. Phys., 50*, 197–206, 1988.

Lall, U., and M. E. Mann, Low frequency climatic variability: Inferences from the Great Salt Lake (abstract), *Eos Trans. AGU, 74*, 123, 1993.

Lall, U., and Y. Moon, Large scale atmospheric indices and Great Salt Lake: Interannual and Interdecadal variability (abstract), *Eos Trans. AGU, 75*, 21, 1994.

Latif, M., and T. P. Barnett, Causes of Decadal Climate Variability over the North Pacific and North America, *Science, 266*, 634–637, 1994.

Lins, H. F., Streamflow variability in the United States, 1931–78, *J. Clim. and Appl. Met., 24*, 463–471, 1985.

Lins, H. F., and P. J. Michaels, Increasing U.S. streamflow linked to greenhouse forcing, *Eos Trans. AGU, 75*, 281–285, 1994.

Mann, M. E., and J. Park, Spatial correlations of interdecadal variation in global surface temperatures, *Geophys. Res. Lett., 20*, 1055–1058, 1993.

Mann, M. E., and J. Park, Global-scale modes of surface temperature variability on interannual to century timescales, *J. Geophys. Res., 99*, 25819–25833, 1994.

Mehta, V. M., and T. Delworth, Decadal variability in the tropical Atlantic Ocean surface temperature in shipboard measurements and a global ocean-atmosphere model, *J. Clim.* (in press), 1994.

Park, J., and K. A. Maasch, Plio-Pleistocene time evolution of the 100-kyr cycle in marine paleoclimate records, *J. Geophys. Res., 98*, 447–461, 1993.

Rasmusson, E. M., and P. A. Arkin, A global view of large-scale precipitation variability, *J. Clim., 6*, 1495–1522, 1993.

Thomson, D. J., Spectrum estimation and harmonic analysis, *IEEE Proc., 70*, 1055–1096, 1982.

Trenberth, K. E., Recent interdecadal climate changes observed in the northern hemisphere, *Bull. Am. Meteorol. Soc., 71*, 988–993, 1990.

Weaver, A. J., E. S. Sarachik, and J. Marotzke, Freshwater flux forcing of decadal and interdecadal oceanic variability, *Nature, 353*, 836–838, 1991.

Willett, H. C. and J. T. Prohaska, The prediction of the future water levels of the Great Salt Lake, in *Cenozoic Geology of Western Utah-Sites for precious metal and hydrocarbon accumulations*, pp. 229–237, Utah Geological Association, Salt Lake City, UT., 1987

M. E. Mann, Department of Geology and Geophysics, Kline Geology Laboratory, P.O. Box 208109, New Haven, CT 06520-8109.

(Received November 23, 1994; revised January 16, 1995; accepted February 13, 1995.)